The Role of Diffusivity Changes on The Pattern of Warming in Energy Balance Models

Chiung-Yin Chang, [a] , Timothy M. Merlis, [a]

[a] *Program in Atmospheric and Oceanic Sciences, Princeton University, Princeton, New Jersey*

ABSTRACT: Atmospheric macroturbulence transports energy down the equator-to-pole gradient. This is represented by diffusion in energy balance models (EBMs), and EBMs have proven valuable to understanding and quantifying the pattern of surface temperature change. They typically assume climate-state independent diffusivity, chosen to well represent the current climate, and find that this is sufficient to emulate warming response in general circulation models (GCMs). Here, we examine the role that changes in diffusivity play in the large-scale equator-to-pole contrast in surface warming in EBMs, motivated by theories for polar amplified warming. New analytic theories for two formulations of climate-state dependent diffusivity successfully capture the results of numerical EBM solutions. While existing GCM studies do not agree on the sign of simulated diffusivity changes with warming, they have never found enough diffusivity reduction to eliminate polar amplified warming. For reasonable choices of parameter values, the success of the new analytic theories reveals why.

1. Introduction

Atmospheric macroturbulence plays a leading-order role in determining the meridional distribution of temperature. A simple conceptual picture is to consider this large-scale turbulence as acting to transport energy down the equator-to-pole energy gradient, a downgradient diffusion. One application of the diffusive picture is to use it as a turbulence closure and avoid explicitly simulating atmospheric motions in energy balance models (EBMs). Here, the radiative fluxes are typically linear functions of surface temperature, as in climate feedback analysis, and the atmospheric energy transport is governed by the gradient of temperature (dry EBMs) or moist static energy (moist EBMs).

Recently, moist EBMs have been used to emulate the temperature change pattern of comprehensive climate models with prescribed radiative feedback parameters and surface fluxes to the ocean (Armour et al. 2019; Russotto and Biasutti 2020; Hill et al. 2022). There has also been theoretical understanding of these EBMs (Flannery 1983; Merlis and Henry 2018) for radiatively forced climate change, highlighting the role that additional latent energy transport with warming can play in polar amplification. While much of EBM research has focused on the role of the spatial pattern of radiative feedbacks or the role of moisture in energy transport changes, there has been relatively limited analysis of cases with non-constant diffusivity.

Most EBM research that seeks to emulate the behavior of general circulation model (GCM) simulations has neglected potential changes of diffusivity despite that diffusivities are known to change in these higher rung of

Corresponding author: Chiung-Yin Chang, cychang@princeton.edu

models (Hwang and Frierson 2010; Roe et al. 2015; Armour et al. 2019). Aquaplanet atmospheric GCM simulations simulate decreases in the midlatitude diffusivities in response to uniform surface warming (Shaw and Voigt 2016), but the midlatitude maximum may increase (Mooring and Shaw 2020). Lu et al. (2022) has $\approx 3\%$ reduction in diffusivity at $45°$ in GCM simulations of the response to doubled CO_2 that allow for meridional temperature gradients to weaken. Finally, the coupled model simulations analyzed by Wu et al. (2011) show increases in diffusivity in both hemispheres in a DJF average of a transient warming scenario (their Fig. 6). We also note that the diffusivity may vary non-monotonically with global mean temperature (O'Gorman and Schneider 2008) and diffusive theories developed for GCM simulations of climate change do require to climate-state dependent formulations to capture the behavior over a wide range of climates (Frierson et al. 2007; Bischoff and Schneider 2014; Merlis et al. 2022; Lu et al. 2022).

Existing theories for the diffusivity $\mathcal{D}$ have indeed suggested a variety of climate-state dependent formulations and there remains no agreement on a widely accepted form that nicely describes the behavior of Earth's atmosphere. The starting point for these theories may be based on (quasi-)linear baroclinic instability theory (Green 1970; Stone 1972; Schneider 2006) or fully developed quasi-geostrophic turbulence thoery (Held and Larichev 1996; Barry et al. 2002; Chang and Held 2022), but their common goal is to seek for a closure that expresses the diffusivity as a function of forcing and planetary parameters, or at least the environmental variables. Given the baroclinic nature of atmospheric macroturbulence, these variable are naturally the vertical wind shear and deformation radius, or equivalently temperature gradient $\partial_y T$ and static stability $\partial_z T$, in dry atmospheres. Since typical EBMs do not contain a

vertical dimension, it is then the quantitative dependence [e.g., the power law dependence of $\mathcal{D} \propto (\partial_y T)^k$] that vary among the different dry diffusivity theories of relevance to EBM theory.

Any attempt to extend the dry theories and further consider the role of water vapor is however difficult, as the presence of moisture and the associated latent energy release may fundamentally alter the underlying dynamics (Frierson et al. 2007; O'Gorman and Schneider 2008). From a global entropy budget perspective, Chang and Held (2022) hypothesized that, so long as it is the diffusion of moist enthalpy of interest, the corresponding diffusivity would likely depend on moist enthalpy gradient as well. In the context of moist EBM theory, this suggests that the diffusivity may depend on the moist static energy (MSE) gradient in addition to the temperature gradient. It is therefore interesting to ask if the diffusivity in moist EBMs is made to vary with climate states, how the warming pattern—polar amplification in particular —is affected. Addressing this question is valuable in that it helps bound the errors associated with neglecting climate-state dependent diffusivity, as this is the little-scrutinized, standard practice in the previous work.

Here, we build on the analytic moist EBM theory developed by Merlis and Henry (2018, hereafter MH18) to offer new analytic progress on understanding how changing diffusivity impacts the pattern of warming. Motivated by the diffusivity dependences identified in previous GCM simulations and proposed by existing scaling theories, we consider two climate-state dependent forms of diffusivity. The first depends linearly on global mean temperature and the second scales with the temperature and MSE gradients with some power law dependence. In what follows, we present the EBM formulation and review the theoretical results of MH18 in section 2, analyze the results for a global mean temperature dependent diffusivity in section 3, analyze the results for temperature- and MSE-gradient dependent diffusivities in section 4, discuss the relationships of our results and previous studies in section 5, and offer conclusions in section 6.

2. Energy Balance Models

a. Governing Equation

The diffusive EBM is governed by a one-dimensional partial differential equation

$$C\partial_t T(\phi) = \frac{1}{4}QS(\phi)a(\phi) - [A + BT(\phi)] - \nabla \cdot \mathbf{F_a}(\phi) + \mathcal{F},$$
(1)

with heat capacity C, surface temperature T, latitude ϕ, solar constant $Q = 1360\,\mathrm{W\,m^{-2}}$, insolation structure function $S(\phi)$, co-albedo $a(\phi)$, outgoing longwave radiation OLR $= A + BT$, atmospheric energy flux divergence $\nabla \cdot \mathbf{F_a}$, and radiative forcing $\mathcal{F}$.

Here, we are focused on the role of climate-dependent diffusivity, so we keep the radiation simple. For the shortwave, the insolation is time independent and similar to Earth's annual-mean, and the co-albedo is a climate-state independent function that captures the structure of Earth's annual-mean planetary albedo, as in North et al. (1981). For the longwave, both components of the outgoing longwave radiation have constant parameter values of $A = 281.67\,\mathrm{W\,m^{-2}}$ and the longwave feedback parameter that is spatially uniform with a value of $B = 1.8\,\mathrm{W\,m^{-2}\,K^{-1}}$. The radiative forcing that we use is spatially uniform with a value $\mathcal{F} = 3.6\,\mathrm{W\,m^{-2}}$, inspired by the global-mean radiative forcing of a doubling of CO_2. We emphasize that we are not prescribing spatially varying forcing, feedbacks, or ocean heat uptake to emulate comprehensive GCMs (Armour et al. 2019; Russotto and Biasutti 2020; Beer and Eisenman 2022; Hill et al. 2022).

The divergence of the atmospheric energy flux is governed by diffusion of MSE: $\nabla \cdot \mathbf{F_a} = -\partial_x[\mathcal{D}(1 - x^2)\partial_x h]$, with $x = \sin\phi$, diffusivity $\mathcal{D}$, and MSE defined in units of temperature $h = T + L\mathcal{H}c_p^{-1}q^*(T)$. The relative humidity $\mathcal{H}$ is spatially constant with a standard value of 0.8. Setting $\mathcal{H}$ to zero converts the moist EBM to a dry EBM.

To keep the analysis straight forward, we consider variants of the EBM with a spatially constant $\mathcal{D}$ and vary its value either as the global-mean temperature or as simple functions of the equator-to-pole temperature and/or MSE contrast evaluated as the coefficients of Legendre polynomials. Legendre polynomials are a set of orthogonal basis functions for the sphere and a series solution to the EBM governing equation has been widely used (North 1975, MH18). The order of the Legendre polynomials is indicated by subscripts, and the two of interest here are the zeroth (the global mean, e.g., T_0) and second order [the coefficient T_2 that multiplies the polynomial $(3x^2 - 1)/2$].

In addition to a climate-invariant diffusivity, we introduce one category climate-state dependent diffusivity of the form:

$$\mathcal{D}(T_0) = \overline{\mathcal{D}}[1 + \gamma(T_0 - \overline{T}_0)],$$
(2)

where the temperature sensitivity of the diffusivity γ for a global-mean temperature change can be expressed in percent per kelvin for comparison to that of the Clausius-Clapeyron (CC) relation. Throughout, $\overline{(\cdot)}$ indicates a control climate value.

One can motivate the $\mathcal{D}(T_0)$ analysis from an uncertainty quantification perspective: a standard moist EBM formulation has a spatially constant and climate invariant diffusivity. Our aim is to evaluate the neglect of climate-state dependent diffusivity on the pattern of warming. The logical starting point for this quantification is to examine the sensitivity of a diffusivity that varies in proportion to the global-mean temperature $\mathcal{D}(T_0)$. One can think of this as encapsulating the net effect of other aspects of the climate statistics that may more directly determine the dif-

fusivity $\mathcal{D}$. So, we extend the analytic EBM theory to this case.

The other category of climate-state dependent diffusivity that we consider responds to gradients. As discussed in the introduction, given the lack of consensus on the particular power law that quantitatively captures the dependence of the diffusivity on the meridional temperature or MSE contrast, we provide a theory for the general case. The state variable of the EBM is surface temperature and the derived quantity surface MSE is, of course, readily available. As there is no vertical information available, we must assume that the diffusivity is proportional to these surface quantities that are available and then modify the exponent. In other words, we assume there is a relationship between the vertically varying information (like isentropic slopes) that appears in diffusivity theories and the surface variables of the EBM. The most general expression for meridional contrast dependent diffusivity is then a power law function of T_2 and h_2 relative to their control values:

$$\mathcal{D}(T_2, h_2) = \overline{\mathcal{D}} \left(\frac{T_2}{\overline{T}_2}\right)^n \left(\frac{h_2}{\overline{h}_2}\right)^m. \tag{3}$$

As the exponent is raised, the sensitivity of the diffusivity to the contrast increases. For example, a weakened temperature gradient relative to that of the control climate, $0 > T_2 > \overline{T}_2$, implies a larger reduction of $\mathcal{D}$ from the control $\overline{\mathcal{D}}$ if $n > 0$ and n is large. Again, we emphasize that the T_2 or h_2 dependence is modifying the magnitude of the spatially uniform diffusivity and does not, for example, give it a specific form of spatial dependence.

The control value of the diffusivity is $\overline{\mathcal{D}} = 0.3\,\mathrm{W\,m^{-2}\,K^{-1}}$. The overall moist EBM configuration is identical to MH18. Given that we are interested in equilibrium solutions, our analysis is focused on $\partial_t T = 0$, and we compare them to numerical steady states obtained via time-marching of the above equation [with details as in MH18]. There are 180 grid points that are evenly spaced in x for a domain that spans both hemispheres. The control numerical solution has global-mean surface temperature of $288.6\,\mathrm{K}$ and an equator-to-pole difference of $46.5\,\mathrm{K}$. The second-order Legendre polynomial component of the temperature $\overline{T}_2$ is $-29.3\,\mathrm{K}$ and of the MSE $\overline{h}_2$ is $-65.4\,\mathrm{K}$, which are negative because both *decrease* from equator to pole. We use these second-order Legendre polynomial components as the relevant metric for large-scale gradients and describe temperature change patterns as polar amplified based on this measure.

b. Analysis Approach and Response to Warming with Constant Diffusivity

In this section, we briefly review the central theoretical result of MH18 and show the numerical EBM solution response to radiative forcing for the spatially constant and climate-state independent diffusivity moist EBM.

To derive EBM theories for the pattern of temperature change, we follow the approach of MH18, who built on dry EBM theories (North 1975; North et al. 1981). The governing equation is expanded spectrally in Legendre polynomials and truncated to find solutions. The global-mean (order zero polynomial) and second-order Legendre polynomial component account for much of the meridional structure of the temperature change pattern (sometimes known as a "two-mode solution"). MH18 presented these solutions for moist EBMs with spatially constant feedback and diffusivity and either spatially varying or constant radiative forcing.

The essence of the analysis approach for moist EBMs is to approximate the MSE h in terms of temperature via Taylor series expansion. This expansion can be done about a spatially varying climatological surface temperature distribution [MH18 Eq. (12)] or about the global-mean surface temperature [MH18 Eq. (14)]. Here, we adopt the later approach. It is simpler, makes analysis feasible, and the error it introduces is modest.

Our approximate MSE $\tilde{h}$ is defined as:

$$\tilde{h} \equiv T + L\mathcal{H}c_p^{-1}[q^*(\overline{T}_0) + \partial_T q^*|_{\overline{T}_0}(T_0 - \overline{T}_0)]. \tag{4}$$

The appeal of linearizing the definition of q^* about the global-mean temperature T_0 rather than the spatially varying climatology is that it eliminates the spatial derivatives of the linearized q^*: $\partial_x \tilde{h} = (1 + L\mathcal{H}c_p^{-1}\partial_T q^*|_{T_0})\partial_x T$. After inserting this definition of MSE $h = \tilde{h}$ into the steady-state EBM governing equation Eq. (1), we have:

$$0 = \frac{1}{4}QSa - (A + BT) - \partial_x[\mathcal{D}(1 + L\mathcal{H}c_p^{-1}\partial_T q^*|_{\overline{T}_0})(1 - x^2)\partial_x T]. \tag{5}$$

So, we can think of the role of latent energy as changing the magnitude of the diffusivity. Collecting terms at second order and specifying the climate-state independent diffusivity $\mathcal{D} = \overline{\mathcal{D}}$, we have:

$$T_2 = \frac{\frac{1}{4}Q(Sa)_2}{6\overline{\mathcal{D}}(1 + L\mathcal{H}c_p^{-1}\partial_T q^*|_{\overline{T}_0}) + B}, \tag{6}$$

where the factor of 6 results from the eigenvalue of the eigenfunction for the diffusion operator. This expression shows that the climatological T_2 is negative because the numerator is negative: there is less absorbed solar radiation in the high latitudes than in the low latitudes.

The sensitivity of this expression to global-mean surface temperature T_0 change can be obtained with an application of the chain rule in evaluating the derivative of Eq. (6):

$$\frac{\partial T_2}{\partial T_0} = \frac{-6\overline{\mathcal{D}}\,\overline{T}_2 L\mathcal{H}c_p^{-1}\partial_{TT}q^*|_{\overline{T}_0}}{6\overline{\mathcal{D}}(1 + L\mathcal{H}c_p^{-1}\partial_T q^*|_{\overline{T}_0}) + B}. \tag{7}$$

This expression is similar to Eq. (14) of MH18, who gave numerical values for representative values of Earth that imply about 2.8 times as much warming at the pole relative to the equator. [There is a modest difference in that their Eq. (14) required an integral to compute a modification of the diffusivity due to latent energy that appears in that denominator, but it has a similar numerical value as the product of the term in parenthesis, $1 + L\mathcal{H}c_p^{-1}\partial_T q^*|_{\overline{T}_0}$, in the denominator here.] One can see that this equation has a positive-definite denominator and numerator ($\overline{T}_2 < 0$, all other terms > 0). Therefore, $\partial_{T_0}T_2 > 0$ and there is always a reduction of the magnitude of T_2 with warming. That is, the temperature gradients weaken with warming, regardless of the parameter values used to evaluate the expression.

Another appeal of adopting the approximate MSE $h = \tilde{h}$ in Eq. (4) is that we can also derive the analytic expression for the sensitivity of MSE contrast h_2 to T_0 change. Using Eq. (4), we can simply express

$$h_2 = (1 + L\mathcal{H}c_p^{-1}\partial_T q^*|_{\overline{T}_0})T_2 \qquad (8)$$

and apply the product rule to obtain the relationship between h_2 and T_2 sensitivities:

$$\frac{\partial h_2}{\partial T_0} = (1 + L\mathcal{H}c_p^{-1}\partial_T q^*|_{\overline{T}_0})\frac{\partial T_2}{\partial T_0} + \overline{T}_2 L\mathcal{H}c_p^{-1}\partial_{TT}q^*|_{\overline{T}_0}, \qquad (9)$$

Inserting the $\partial_{T_0}T_2$ expression in Eq. (7) into this gives

$$\frac{\partial h_2}{\partial T_0} = \frac{B\overline{T}_2 L\mathcal{H}c_p^{-1}\partial_{TT}q^*|_{\overline{T}_0}}{6\overline{\mathcal{D}}(1 + L\mathcal{H}c_p^{-1}\partial_T q^*|_{\overline{T}_0}) + B}. \qquad (10)$$

Similar to Eq. (7), one can see that this equation is negative definite. That is, $\partial_{T_0}h_2 < 0$ and the MSE gradients always enhance with warming. Given that $\mathcal{D} = \overline{\mathcal{D}}$ is assumed climate invariant, this also guarantees an increased poleward energy transport, which was argued as the essential driver for polar amplification by MH18. For the same reason, MH18 concluded that applying the uniform MSE increase approximation of Byrne and O'Gorman (2013) over all latitudes cannot be a self-consistent solution in this EBM formulation.

The estimate from these approximate analytic expressions and the numerical solution is compared in Figure 1. For $\mathcal{F} = 3.6\,\mathrm{W\,m^{-2}}$, which corresponds to a global mean temperature change $\Delta T_0 = T_0 - \overline{T}_0 = 2\,\mathrm{K}$ (where Δ indicates the difference from the control climate value), Figure 1a shows the numerical solution and the theory, $\partial_{T_0}T_2$ from Eq. (7) times ΔT_0, for the pattern of the temperature change (black solid and dashed lines, respectively). The theory modestly underestimates the T_2 component of the warming, as also indicated by its slight overestimate of ΔT_2 with $\gamma = 0$ in Fig. 1b. Likewise, there is a small discrepancy between the numerical solution and Eq. (10) times ΔT_0 for the Δh_2 value with $\gamma = 0$ that can be seen in Fig. 1c.

Having set up the definition of approximate MSE that we will use in subsequent analysis and reviewed the result of MH18 for climate-invariant diffusivity, we turn to the climate-state dependent diffusivity formulations.

3. Global-mean Temperature Dependent Diffusivity

Given that the moist EBM theory with constant diffusivity has polar amplified warming, we investigate how it would change with a global-mean temperature dependent diffusivity [Eq. (2)]: $\mathcal{D} = \mathcal{D}(T_0)$.

a. Numerical Results

We show the surface temperature change using a global-mean temperature dependent diffusivity Eq. (2) in Fig. 1a. The typical, climate-state independent diffusivity $\gamma = 0$ has polar amplified warming with about 2.5 times as much polar warming as in the global mean (black line in Fig. 1a). Increased diffusivity with warming ($\gamma > 0$, blue line in Fig. 1a), has further enhanced polar warming. As the diffusivity is decreased with warming, there is less enhancement of the polar warming (progressively darker shades of solid red lines in Fig. 1a are more negative γ). There is a transition from polar to tropically amplified warming that occurs with a diffusivity that decreases with global-mean surface temperature somewhere between the $-2\%\,\mathrm{K^{-1}}$ and $-4\%\,\mathrm{K^{-1}}$ cases plotted. Our theoretical developments focus on the sensitivity of the T_2 component of the EBM solution, but we note that there can be higher-order spatial structure in the numerical EBM solutions. The numerical EBM solutions plotted that have the strongest reductions in the diffusivity with warming show weak spatial variations in the warming pattern from the equator to $\approx 40°$ and a subseqent steep drop in temperature. This is an indication that there is a fourth-order Legendre polynomial component of the temperature change.

Figure 1b shows the numerical EBM's ΔT_2 in circles against the diffusivity's temperature sensitivity γ. As γ becomes more negative, ΔT_2 decreases linearly. We see here that the transition from positive ΔT_2 (polar amplified warming) to negative ΔT_2 (tropically amplified warming) occurs near $\gamma = -3\%\,\mathrm{K^{-1}}$.

Figure 1c shows the numerical EBM Δh_2 in circles vs. γ. For most of the values of γ, Δh_2 is negative. This indicates an increased meridional moist static energy contrast. The exception occurs for the largest magnitude increase in diffusivity with global-mean temperature. The response of h_2 to warming varies approximately linear in γ, which the theory that we derive next can account for.

b. Theory

The start of the analysis proceeds as in section 2b. The EBM governing equation now becomes Eq. (5) with $\mathcal{D}\mathcal{D}(T_0)$ defined by Eq. (2). Compared to the $\mathcal{D} = \overline{\mathcal{D}}$
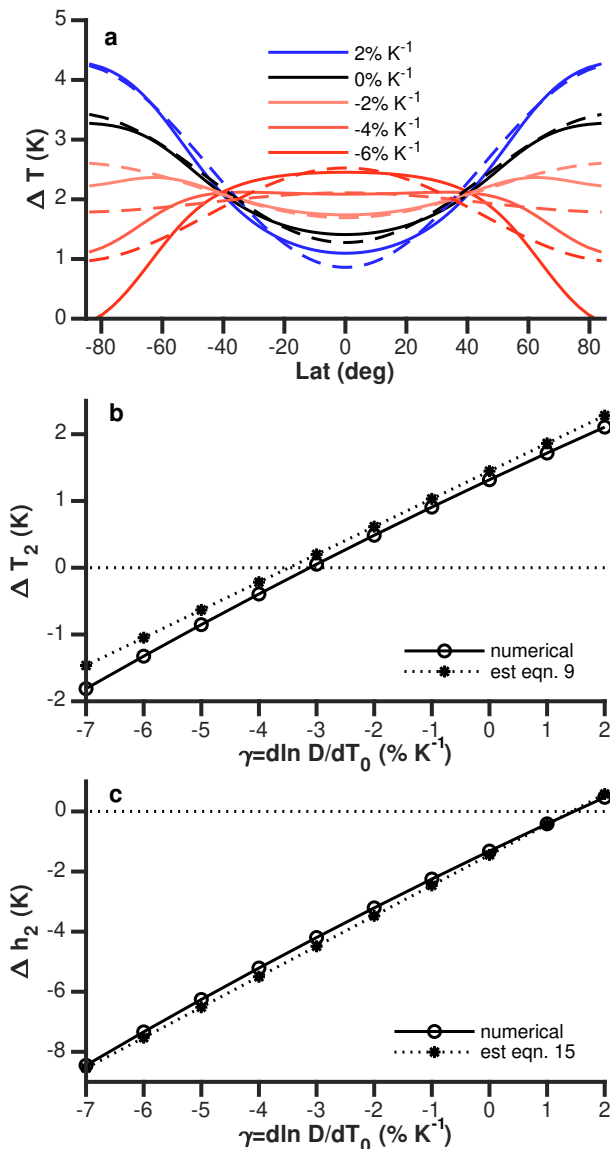
FIG. 1. (a) Change in surface temperature vs. latitude for numerical EBM solutions (solid lines) and analytic theory [Eq. (12) scaled by the global-mean temperature change ΔT_0, dashed lines] for global-mean temperature dependent diffusivity [Eq. (2)] with sensitivity coefficients indicated in the caption. (b) Change in the second-order Legendre polynomial component of temperature T_2 vs. diffusivity sensitivity coefficient γ for numerical EBM solutions and the analytic theory [Eq. (12)]. (c) Change in the second-order Legendre polynomial component of moist static energy h_2 vs. diffusivity sensitivity coefficient γ for numerical EBM solutions and the analytic theory [Eq. (17)].

solution for the T_2 component of temperature in Eq. (6), the $\mathcal{D} = \mathcal{D}(T_0)$ solution now has an additional modification to the diffusivity in the denominator (beyond the one from the latent energy component of the MSE) that results

from its T_0 dependence:

$$T_2 = \frac{\frac{1}{4}Q(Sa)_2}{6\overline{\mathcal{D}}\{[1 + \gamma(T_0 - \overline{T}_0)](1 + L\mathcal{H}c_p^{-1}\partial_T q^*|_{\overline{T}_0})\} + B}. \tag{11}$$

This additional T_0-dependent term in the denominator of Eq. 11 that results from the temperature-dependent diffusivity gives rise to a new term in the numerator of the expression for the T_2 sensitivity to a global-mean temperature change:

$$\frac{\partial T_2}{\partial T_0} = \frac{-6\overline{T}_2\overline{\mathcal{D}}[L\mathcal{H}c_p^{-1}\partial_{TT}q^*|_{\overline{T}_0} + \gamma(1 + L\mathcal{H}c_p^{-1}\partial_T q^*|_{\overline{T}_0})]}{6\overline{\mathcal{D}}(1 + L\mathcal{H}c_p^{-1}\partial_T q^*|_{\overline{T}_0}) + B}. \tag{12}$$

This theory is compared to the numerical EBM solutions in Fig. 1a,b. It captures the linear γ-dependence of ΔT_2 (Fig. 1b), though there is some higher-order structure that it can not when compared latitude by latitude (Fig. 1a dashed vs. solid lines).

The theory has a critical diffusivity sensitivity $\gamma = \gamma_{c,T}$ for which there is no change in T_2 with global warming T_0. This is the boundary between simulations with polar amplified and tropically amplified warming. Setting the quantity in square brackets in Eq. (12) to zero, results in

$$\gamma_{c,T} = -\frac{L\mathcal{H}c_p^{-1}\partial_{TT}q^*|_{\overline{T}_0}}{1 + L\mathcal{H}c_p^{-1}\partial_T q^*|_{\overline{T}_0}}. \tag{13}$$

For Earth values, this expression suggests a critical diffusion coefficient sensitivity of $\gamma_{c,T} \approx -3\% \text{K}$. Consistent with our theory, the numerical EBM's ΔT_2 changes from positive (polar amplified) to negative (tropically amplified) for $\gamma < -3\% \text{K}^{-1}$ (Fig. 1b).

We offer two related interpretations for the form and climatological dependence of $\gamma_{c,T}$. One is mathematical, and one is physical. Mathematically, the above expression involves the first and second derivative of the saturation specific humidity with respect to temperature. We can make an approximation and assume a pure exponential form of $q^* = q_0^* \exp(\alpha T)$, where α is the CC sensitivity of $\approx 7\% \text{K}^{-1}$. Then, we have an expression for $\gamma_{c,T}$ of the form,

$$\gamma_{c,T} \approx \frac{\kappa\alpha^2}{1 + \kappa\alpha} < \alpha, \tag{14}$$

where κ is a combination of thermodynamic coefficients $L, \mathcal{H}, c_p$, and $q^*|_{\overline{T}_0}$. This expression for $\gamma_{c,T}$ is bound from above by the CC sensitivity α.

A physical picture of what controls $\gamma_{c,T}$ can be obtained by considering the climatological latent vs. sensible energy transports, F_L vs. F_S. Loosely following Held and Soden (2006, their section 5), if we assume both transports are diffusive along its corresponding gradients with the same

diffusivity, their ratio in the EBM is

$$\frac{F_L}{F_S} = L\mathcal{H}c_p^{-1}\partial_T q^*. \tag{15}$$

$$\gamma_{c,T} = -\left(\frac{L\mathcal{H}c_p^{-1}\partial_T q^*}{1 + L\mathcal{H}c_p^{-1}\partial_T q^*}\right)\frac{\partial_{TT}q^*}{\partial_T q^*} = -\left(\frac{F_L}{F_S + F_L}\right)\partial_T\left(\ln\frac{F_L}{F_S}\right) \approx -\left(\frac{F_L}{F_S + F_L}\right)\alpha \tag{16}$$

The last expression is obtained by approximating the temperature sensitivity of $\ln(F_L/F_S)$ as α as discussed above. In this approximate expression, the term in parenthesis, the ratio of latent energy transport and total energy transport, is roughly one-half as the latent and sensible heat transport are about the same in Earth's mid-latitudes. In other words, the pre-factor of α is set by how much energy transport is from the latent component in the control cli-

We use this ratio to express $\gamma_{c,T}$ in terms of climatological ratios of sensible and latent transports, as follows:

mate. The more dominant the latent transport is, the more the diffusivity has to decrease to fight against it to prevent polar-amplified warming.

Next, we use the theory for T_2 to quantify MSE contrasts. As for Eq. (10), but inserting the $\partial_{T_0}T_2$ expression of Eq. (12) into Eq. (9) gives

$$\frac{\partial h_2}{\partial T_0} = \overline{T}_2 \frac{L\mathcal{H}c_p^{-1}\partial_{TT}q^*|_{\overline{T}_0}}{6\overline{\mathcal{D}}(1 + L\mathcal{H}c_p^{-1}\partial_T q^*|_{\overline{T}_0}) + B}\left[B + 6\overline{\mathcal{D}}(1 + L\mathcal{H}c_p^{-1}\partial_T q^*|_{\overline{T}_0})\frac{\gamma}{\gamma_{c,T}}\right]. \tag{17}$$

This estimate is compared to the numerical EBM solutions in Fig. 1c (dotted vs. solid lines). There is good agreement and one can see that a state of no change in MSE contrast is obtained if the diffusivity increases by $\approx 1.5\%\,\mathrm{K}^{-1}$. This corresponds to another critical diffusivity sensitivity

$$\gamma_{c,h} = -\frac{B}{6\overline{\mathcal{D}}(1 + L\mathcal{H}c_p^{-1}\partial_T q^*|_{\overline{T}_0})}\gamma_{c,T} \tag{18}$$

such that the terms in square brackets of Eq. (17) sum to zero. For the climatological values, the ratio of B to $6\overline{\mathcal{D}}(1 + L\mathcal{H}c_p^{-1}\partial_T q^*|_{\overline{T}_0})$ is about one half, so $\gamma_{c,h} \approx +1.5\%\,\mathrm{K}^{-1}$ produces a state of approximately unchanged MSE contrast. Physically, this ratio represents the relative efficiency of the system to damp an imposed radiative forcing via OLR locally or through the meridional spread by diffusive transport. The less efficient the OLR relative to the diffusive transport, the more the anomalous MSE contrast is smoothed out by the turbulent diffusion and the less h_2 changes.

As noted in section 2b, MH18 presented an estimate for polar amplification inspired by Byrne and O'Gorman (2013) that assumed uniform Δh at all latitudes and determined the warming pattern to achieve that state. There, they noted that this solution does not satisfy the energy balance of climate-state invariant diffusivity moist EBM [i.e., Eq. (10)], as it would require an unchanged energy transport. Here, we see that a uniform Δh can do satisfy the EBM equation if diffusivity changes with global-mean temperature in this specific way. This unchanged

h_2 warmed climate has large increases in T_2 (substantially enhanced transport and the concomitantly large PA) helps build intuition for some of the climate-state dependent diffusivities that depend on gradients considered in the next section.

4. Temperature and Energy Gradient Dependent Diffusivity

In this section, we present numerical results and analytic theory for diffusivities that depend on either or both of the second-order Legendre polynomial component of temperature and MSE [Eq. (3): $\mathcal{D} = \mathcal{D}(T_2, h_2)$. The exponent n controls the T_2 dependence of the diffusivity and the exponent m controls the h_2 dependence of the diffusivity. We consider $m = 0$ and vary n to examine how this representation of temperature contrast-dependent diffusivity affects the EBM solution, as well as the case with diffusivity dependent solely on MSE contrast ($n = 0$ with varied m). Last, we examine the case of combined dependence with equal exponents.

We note that the analytic EBM theory developed in the following is general, so the previous literature is largely used to shape our choices of parameters for the calculations of numerical EBM solutions. Our overview here sets aside the exact definitions for how the temperature or MSE gradients are evaluated and focuses on the power laws: Frierson et al. (2007) proposed that $\mathcal{D}$ scales with the 3/2th power law of temperature gradient [their Eq. (A6)], which suggests $n = 3/2$. Lu et al. (2022) proposed

that $\mathcal{D}$ scales with the 3rd power law of temperature gradient [their Eq. (A13a)], which suggests $n = 3$. Chang and Held (2022) generalized the theories of Held and Larichev (1996) and Barry et al. (2002) [their Eq. (29)]. They showed that Held and Larichev (1996) theory corresponds to a special case of dry atmospheres with the mixing slope approximated by isentropic slope, and an additional constant isentropic slope assumption would suggest $n = 3/2$. For moist atmospheres, they suggest $m = n = 3/2$, if the temperature gradient along the mixing slope is assumed to scale with horizontal temperature gradient, following Barry et al. (2002)'s assumption. Certain choices (e.g., exclusively h_2 dependent diffusivity, $m > 0$ with $n = 0$) have never been suggested, but are useful to build intuition for the roles of the individual components of the combined T_2- and h_2-dependent diffusivity case. In all cases, we consider $m \geq 0$ and $n \geq 0$.

a. Numerical results

Figure 2a shows the temperature change vs. latitude for the numerical solution of the EBM with diffusivity dependent on T_2 only ($m = 0$): $\mathcal{D}(T_2)$. We plot select exponents of the power law dependence ($n = 3/2$ and $n = 3$). As the exponent increases from zero (shown in black), there is a reduction in PA. This is expected from the stabilizing feedback: polar amplification provoked initially tends to increase T_2 from its negative control value, and this, in turn, decreases the diffusivity, which reduces the increase in meridional MSE transport that underlies polar amplification in this EBM configuration. Figure 2b shows the systematic variation of the exponent. The change in T_2 decreases from $\approx 1.3\,\mathrm{K}$ to $\approx 0.4\,\mathrm{K}$ as n increases from 0 to 3 and remains positive in all cases. Our analysis will, indeed, reveal that larger exponents cannot change the sign of ΔT_2. Figure 2f shows the diffusivity decrease is $\approx 5\%$ for the highest exponent. Fig. 2d shows h gradients increase with n: the more uniform ΔT, has relatively stronger MSE gradients and this is a countervailing tendency for reduced energy transport as the diffusivity decreases ($\Delta \mathbf{F_a} \sim \overline{D}\partial_x \Delta h + \Delta D \partial_x \overline{h}$). A central appeal of the analysis of the next section is that these competing effects are quantitatively captured via the analysis of the EBM's governing equation.

Figure 2c shows the temperature change vs. latitude for the numerical solution of the EBM with diffusivity de-

pendent on h_2 only ($n = 0$): $\mathcal{D}(h_2)$. This form of the climate-state dependent diffusivity has an increase in polar amplification as the exponent increases. Here, the feedback associated with the diffusivity is as follows: the initial response tends to decrease h_2 [more negative relative to the negative $\overline{h}_2$, Eq. (10)], this in turn, increases the diffusivity (Fig. 2f), augmenting the increase in meridional MSE transport that underlies the PA. The higher exponent approaches the uniform Δh limit (Fig. 2d). Figure 2b shows the systematic variation of the exponent, revealing that the change in T_2 reaches $\approx 1.6\,\mathrm{K}$ (about 25% more polar amplification than the climate-state independent diffusivity). The contrast between the behavior of T_2-dependent diffusivity (orange in Fig. 2) and h_2-dependent diffusivity (purple in Fig. 2) is clear: one has decreased diffusivity and weakened polar amplification and the other has increased diffusivity and enhanced PA. This is suggestive that the combined case has more muted changes as a result of these competing effects.

Fig. 2e shows the temperature change vs. latitude for the numerical solution of the EBM with diffusivity dependent on both T_2 and h_2 and $m = n$: $\mathcal{D}(T_2, h_2)$. This form of the climate-state dependent diffusivity has a modest decrease in polar amplification as the exponent increases (brown circles in Fig. 2b). For $m = n = 3/2$, the change in T_2 is $\approx 1.1\,\mathrm{K}$ (about 20% less polar amplification than the climate-state independent diffusivity). There are modest decreases in meridional gradients in MSE and diffusivity as the exponents increase (Fig. 2d,f). These subtle effects result from the competing roles for T_2- vs. h_2-dependent diffusivity changes and provide a stringent test for the theory developed in the next section.

b. Theory

Here, we derive the general case of the EBM's T_2 solution for diffusivities that depend on the combined T_2, h_2-dependent diffusivity [Eq. (3)]. Theories for the individual diffusivity dependencies can be recovered by setting the relevant exponent to zero [e.g., theory for $\mathcal{D}(T_2)$ is given by $m = 0$].

The starting point is, as before, the second-order Legendre polynomial truncation of the EBM governing equation. The approximate definition of MSE $\tilde{h}$ allows us to replace h_2 in the $\mathcal{D}(T_2, h_2)$ expression using Eq. (8). Setting $\mathcal{D}$ in Eq. (5) with this expression results in:

$$0 = \frac{1}{4}Q(Sa)_2 - BT_2 - 6\overline{\mathcal{D}}(1 + L\mathcal{H}c_p^{-1}\partial_T q^*|_{T_0})\left(\frac{1 + L\mathcal{H}c_p^{-1}\partial_T q^*|_{T_0}}{1 + L\mathcal{H}c_p^{-1}\partial_T q^*|_{\overline{T}_0}}\right)^m \left(\frac{T_2}{\overline{T}_2}\right)^{m+n} T_2. \quad (19)$$

Taking the derivative with respective to global-mean temperature T_0, we have

$$\frac{\partial T_2}{\partial T_0} = \frac{-6\overline{T}_2\overline{\mathcal{D}}[L\mathcal{H}c_p^{-1}\partial_{TT}q^*|_{\overline{T}_0}(m+1)]}{6\overline{\mathcal{D}}(1 + L\mathcal{H}c_p^{-1}\partial_T q^*|_{\overline{T}_0})(m+n+1) + B}. \quad (20)$$

Note that this expression is positive definite, in contrast to the corresponding result for the T_0-dependent diffusivity $\mathcal{D}(T_0)$ [Eq. (12)]. The physical meaning of the positive
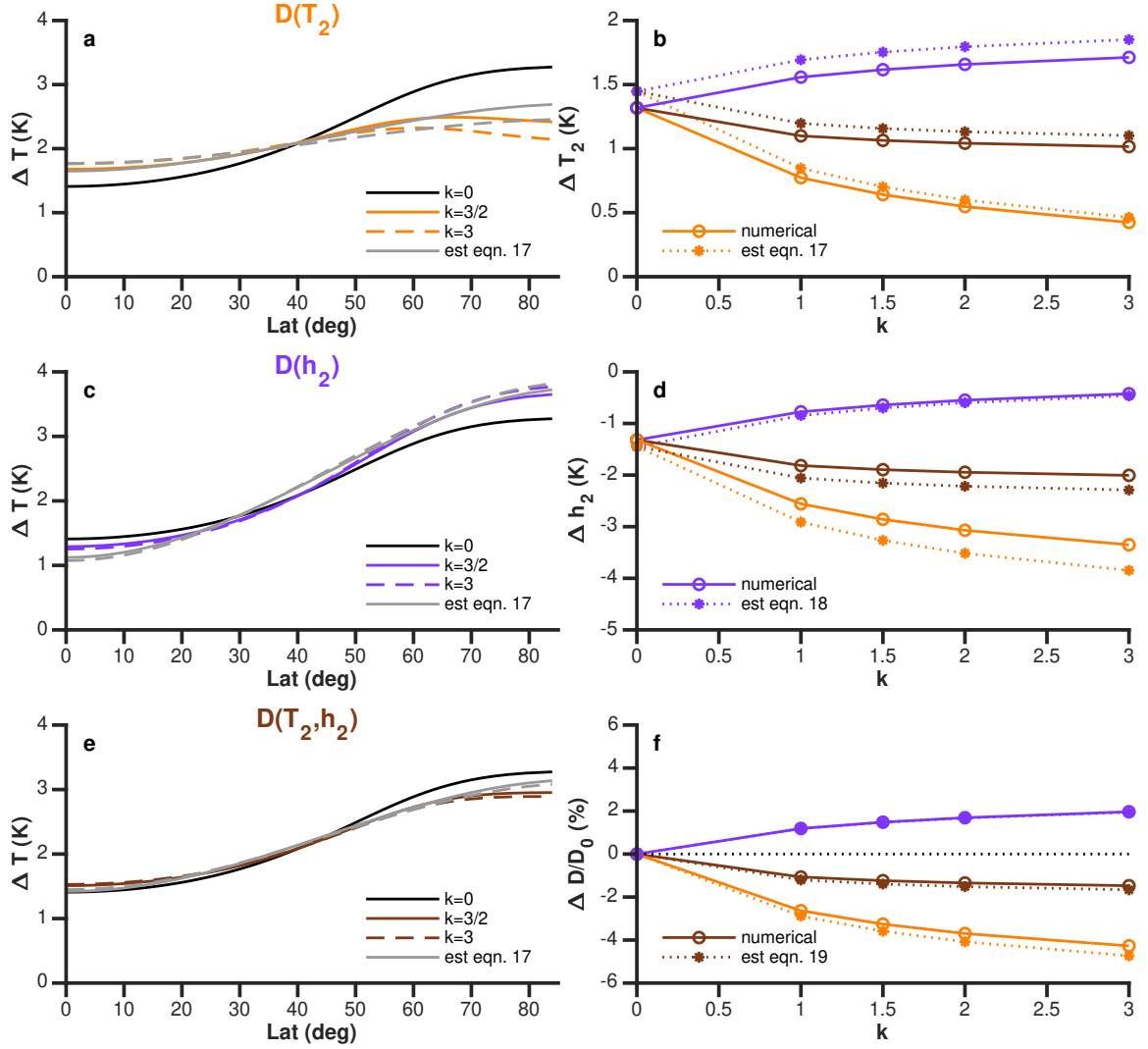
FIG. 2. (a,c,e) Change in surface temperature vs. latitude of T_2 (orange), h_2 (purple), and combined T_2, h_2-dependent (brown) diffusivity for numerical EBM solutions (colored lines) and analytic theory (gray lines) with exponent of Eq. (3) indicated in the legend. (b) Change in the second-order Legendre polynomial component of temperature T_2 vs. diffusivity exponent k for numerical EBM solutions (solid line with open circles) and the analytic theory [dotted line with stars, Eq. (20)]. (d) Change in the second-order Legendre polynomial component of MSE h_2 vs. diffusivity exponent k for numerical EBM solutions and the analytic theory [Eq. (21)]. (f) Percentage change in the diffusivity $\mathcal{D}$ vs. diffusivity exponent k for numerical EBM solutions and the analytic theory [Eq. (22)].

definite expression is that there are *no* parameter values for this form of the climate-state dependent diffusivity that have tropically amplified warming. The limiting case of $n \to \infty$ has $\Delta T_2 \to 0$. That is, polar amplification cannot be eliminated with this diffusivity formulation.

As before, this T_2 sensitivity to T_0 can be used to determine how h_2 varies. When substituting into Eq. (9), we

$$\gamma = \frac{\partial \ln \mathcal{D}}{\partial T_0} = \left(\frac{L\mathcal{H}c_p^{-1}\partial_{TT}q^*|_{\overline{T}_0}}{1 + L\mathcal{H}c_p^{-1}\partial_T q^*|_{\overline{T}_0}} \right) \left[\frac{mB - n6\overline{\mathcal{D}}(1 + L\mathcal{H}c_p^{-1}\partial_T q^*|_{\overline{T}_0})}{6\overline{\mathcal{D}}(1 + L\mathcal{H}c_p^{-1}\partial_T q^*|_{\overline{T}_0})(m+n+1) + B} \right].$$

(22)

have

$$\frac{\partial h_2}{\partial T_0} = \frac{\left[n6\overline{\mathcal{D}}(1 + L\mathcal{H}c_p^{-1}\partial_T q^*|_{\overline{T}_0}) + B \right] L\mathcal{H}c_p^{-1}\partial_{TT}q^*|_{\overline{T}_0}\overline{T}_2}{6\overline{\mathcal{D}}(1 + L\mathcal{H}c_p^{-1}\partial_T q^*|_{\overline{T}_0})(m+n+1) + B}.$$

(21)

This is a negative definite expression, meaning MSE gradients increase with global mean temperature, for all parameter values. For $m \to \infty$, this expression implies $\Delta h_2 \to 0$.

Last, these T_2 and h_2 sensitivity expressions can also be substituted into the $\mathcal{D}(T_2, h_2)$ formula Eq. (3) to derive a theory for the associated diffusivity sensitivity:

The numerator has a difference between m and n: m tends to increase the diffusivity, while n tends to decrease it. Physically, this corresponds to the counteracting effects of increased MSE gradient Eq. (21) and decreased temperature gradient Eq. (20) on the the diffusivity change when T_0 is increased. This competition between the two gradients was speculated by Chang and Held (2022) to limit the warming response of diffusivity, and explain how previous studies using constant-diffusivity EBMs can emulate GCM simulations. The analytic EBM theory here provides a new quantitative description of this competition.

For the case of equal exponents ($m = n$), the diffusivity decreases since the ratio of B to $6\overline{\mathcal{D}}(1 + L\mathcal{H}c_p^{-1}\partial_T q^*|_{\overline{T}_0})$ is about one-half for Earth-like parameter values as discussed before. On the other hand, the upper and lower bounds of the diffusivity sensitivity can be obtained by considering two limiting cases. For $m = 0$ and $n \rightarrow \infty$, $\Delta T_2 \rightarrow 0$ and $\gamma \rightarrow \gamma_{c,T}$. For $n = 0$ and $m \rightarrow \infty$, $\Delta h_2 \rightarrow 0$ and $\gamma \rightarrow \gamma_{c,h}$. Therefore, for $m \geq 0$ and $n \geq 0$, $\gamma_{c,T} < \gamma < \gamma_{c,h}$ is bounded by the two critical diffusivity sensitivities [Eqs. (13) and (18)] discussed in section 3b.

Figure 2 has comparisons of these theories for ΔT_2, Δh_2, and $\Delta \mathcal{D}$ (dotted lines) with the numerical EBM solutions (solid lines). The theories agree well with the numerical EBM solutions. There is some discrepancy in meridional structure for T_2-dependent diffusivity, as the numerical solution has some higher-order components that the theory can not capture (Fig. 2a, gray vs. orange). There is a systematic bias for the ΔT_2 component of the theory [Eq. (20)] and numerical EBM for the $\mathcal{D}(T_2)$ diffusivity (orange dotted vs. solid in Fig. 2b). Likewise, there is a systematic bias for the Δh_2 component of the theory [Eq. (21)] and numerical EBM for the $\mathcal{D}(h_2)$ diffusivity (purple dotted vs. solid in Fig. 2d). Both of these are more modest in the combined T_2, h_2-dependent cases (brown dotted vs. solid in Fig. 2b,d). Overall, the errors of the theory are about $\approx 10\%$ for ΔT_2 and are about $\approx 15\%$ for Δh_2. The numerical solutions' diffusivity changes are well captured by the theory [Eq. (22)] in all cases (Fig. 2f).

5. Discussion

There are some combinations of the moist EBM coefficients (e.g., B, $\mathcal{D}$, and temperature derivatives of q^*) that appear repeatedly in the new analytic formulae. In this section, we introduce two key parameters that encapsulate the EBM theory, shedding light on the origin of the sensitivities derived from the theories and helping to connect them with the theories proposed by previous studies.

First, the relative roles of radiative restoring vs. advective restoring of local energy flux anomalies (two terms with feedback units of $\mathrm{W\,m^{-2}\,K^{-1}}$) is given by μ:

$$\mu \equiv \frac{B}{6\overline{\mathcal{D}}(1 + L\mathcal{H}c_p^{-1}\partial_T q^*|_{\overline{T}_0})}. \qquad (23)$$

It is introduced as it measures the relative importance of the only two energy flux restoring terms that depend on temperature in the climatological global energy balance. It is also one of the nondimensional parameters characterizing the linearized EBM governing equation.

The second parameter (in units of $\mathrm{K^{-1}}$) is

$$\chi \equiv \frac{\partial \ln(1 + L\mathcal{H}c_p^{-1}\partial_T q^*|_{\overline{T}_0})}{\partial T_0} = \frac{L\mathcal{H}c_p^{-1}\partial_{TT}q^*|_{\overline{T}_0}}{1 + L\mathcal{H}c_p^{-1}\partial_T q^*|_{\overline{T}_0}}, \qquad (24)$$

which is introduced as we are interested in the sensitivity to global-mean temperature change and the factor $1 + L\mathcal{H}c_p^{-1}\partial_T q^*|_{\overline{T}_0}$ marks the only nonlinear temperature-dependent term in the governing equation, which fundamentally gives rise to the sensitivity to T_0 in our EBMs.

The sensitivities of T_2, h_2, and $\mathcal{D}$ derived so far can all be recast into functions of μ and χ (Appendix). For instance, the two critical diffusivity sensitivities defined in Eqs. (13) and (18) are effectively $\gamma_{c,T} = -\chi$ and $\gamma_{c,T} = \mu\chi$, respectively. We have provided physical interpretations for them in the above sections, and expressing them in terms of the two key parameters offers an even more parsimonious way to reveal the essential physics.

An advantage of recasting our results in terms of these key parameters is that we can more easily compare our theories to Frierson et al. (2007). Frierson et al. (2007) developed moist EBM theories with climate-state dependent diffusivities to explain the results of a series of idealized GCM simulations where the saturation vapor pressure is modified by a multiplicative factor ξ. This is analogous to replacing q^* by ξq^* in Eq. (1). Assuming a diffusivity that depends on temperature gradient, they showed that their EBM could capture the combination of weakened mean temperature gradients, decreased diffusivity, and increased poleward energy transport as ξ is increased in their GCM simulations. Despite using a different OLR formulation, our EBM theories can offer qualitatively similar predictions for the sensitivities of these aspects of the climates generated by manipulating ξ. The sensitivities to ξ can be obtained by simply replacing χ with $\partial_\xi \ln(1 + L\mathcal{H}c_p^{-1}\partial_T \xi q^*|_{\overline{T}_0})\big|_{\overline{T}_0}$ in the theory derived in section 4b (see also Appendix) with $m = 0$. Accordingly, we recover weakened temperature gradients (increased T_2) and reduced $\mathcal{D}$, while the increase in MSE gradients (decreased h_2) is sufficient to increase the poleward transport as ξ is increased. Frierson et al. (2007) also noted that the OLR and poleward transport in fact barely change with ξ. In our theories, this is equivalent to approaching the $B = \mu = 0$ limit, where the sign of all sensitivities remains the same.

Given that μ characterizes the relative roles of radiative restoring vs. advective (as encapuslated by meridional diffusion) restoring of forcing, it is worth connecting it to a common approach to diagnosing regional temperature change "contributions" from terms in the energy budget

(e.g., Winton 2006; Crook et al. 2011; Pithan and Mauritsen 2014). That local forcing is not entirely locally radiatively restored ($\mu \to \inf$) poses a conceptual challenge to converting energy budgets into temperature change contributions (Merlis 2014): the non-local nature of transport means that regions interact and the budget approach cannot be used quantitatively to anticipate the results of simulations that isolate processes (e.g., feedback locking) or have localized forcing (e.g., regional carbon dioxide concentration changes).

The critical diffusivity sensitivity for the uniform temperature increase $\gamma_{c,T} = -\chi$ has in fact also been derived in Shaw and Voigt (2016). Shaw and Voigt (2016) considered a uniform warming $\Delta T_2 = 0$ and used the approximate MSE definition [their Eq. (3)], which is the same as ours, to derive the corresponding MSE transport [their Eq. (5)]. This can be recovered by Eq. (9) with $\partial_{T_0} T_2 = 0$, which gives $\partial_{T_0} h_2 = \overline{h}_2 \chi$. They next assumed an unchanged energy transport $\Delta(\mathcal{D}h_2) = 0$ and derive the corresponding diffusivity sensitivity to the global mean temperature change [their Eq. (11)]. In our notation, this is $\gamma = \partial_{T_0} \ln \mathcal{D} = -\partial_{T_0} \ln h_2 = -\chi = \gamma_{c,T}$. The crucial difference between the two derivations is that an unchanged energy transport is a direct result following the $\Delta T_2 = 0$ assumption in our EBM formulation (with a uniform B and $\mathcal{F}$). However, an unchanged energy transport is an independent assumption in Shaw and Voigt (2016), motivated by the numerical results of previous GCM studies (e.g., Frierson et al. 2007) rather than global energy balance. As shown in Shaw and Voigt (2016)'s aquaplanet simulations, none of the two assumptions hold even if the model is forced with a prescribed uniform sea surface temperature increase, making any quantitative comparison with their theory difficult.

On the other hand, the diffusivity sensitivity derivedfor diffusivity depends on temperature gradient $\mathcal{D}(T_2)$ [Eq. (22)] does offer a quantitative interpretation for the "reduction ad absurdium" argument put forward in Lu et al. (2022, their section 5a). Specifically, they argued that for a uniform radiative forcing and "in the absence of any strong negative feedback over the polar region", the diffusivity must decrease but can only decrease less than "the CC regulated increase of moisture gradient", if the diffusivity depends on temperature gradient. In our theories (which assume a uniform B and F), this equivalent to setting $m = 0$ in Eq. (22). This states that the diffusivity sensitvity is bounded by $0 > \gamma > \gamma_{c,T} = -\chi$, where the lower bound is the MSE contrast in the limiting case of uniform warming discussed in Shaw and Voigt (2016) and above.

6. Conclusions

There have been many recent applications of moist energy balance models (EBMs) to climate change research

questions. These have started from emulating poleward energy transport (Frierson et al. 2007; Hwang and Frierson 2010) and subsequently centered on the pattern of warming (Armour et al. 2019; Feldl and Merlis 2021; Beer and Eisenman 2022; Hill et al. 2022) and hydrological cycle (Siler et al. 2018; Bonan et al. 2023). The typical assumption is that, to leading order, both the spatial structure of the climatological diffusivity and its changes with warming are negligible. This ansatz seems to persist largely because it gives a reasonable agreement between EBM solutions and GCM simulations rather than being there being solid justifications for the assumption. In parallel, there is a large body of literature on theories of atmospheric diffusivities and diagnosed diffusivity changes in GCM simulations. This suggests the need to directly assess the possible role of diffusivity changes play in EBM solutions of climate change.

Here, we extend the analytic EBM theory for the large-scale temperature gradient developed in Merlis and Henry (2018) to include climate-state dependence of globally uniform diffusivities. As we are focused on the pattern of warming, the theory was developed for diffusivities that depend on the global-mean temperature T_0 and the large-scale temperature and MSE contrasts encapsulated via their second-order Legendre polynomial components, T_2 and h_2, respectively. For both diffusivity formulations, the sensitivities of T_2 and h_2 to T_0 are found to depend on two key parameters: μ [Eq. (23)] and χ [Eq. (24)]. The former measures the relative role of radiative versus diffusive damping on imposed energy flux anomalies, which is introduced as an intrinsic parameter describing the local energy balance in EBMs. The latter measures the nonlinear temperature dependence and the origin of T_0 dependence due to the presence of moisture, which is itself constrained by CC sensitivity and the ratio of the climatological latent to total energy transport. The theory for the warming pattern obtained from the analytic expressions all compare well to numerical EBM solutions.

For the global-mean temperature dependent diffusivity $\mathcal{D} = \mathcal{D}(T_0) \propto \gamma T_0$, two critical values for the prescribed diffusivity sensitivity $\gamma = \partial_{T_0} \ln \mathcal{D}$ are identified: $\gamma = \gamma_{c,T} = -\chi < 0$ [$\approx -3\% K^{-1}$; Eq. (13)] for uniform temperature increase and $\gamma = \gamma_{c,h} = \mu\chi > 0$ [$\approx 1.5\% K^{-1}$; Eq. (18)] for uniform MSE increase. Each has corresponded to a baseline calculation for the warming response. The uniform temperature increase was argued by Shaw and Voigt (2016) to be a natural starting point to estimate the diffusivity response to warming. Accordingly, they derived the diffusivity dependence on global mean temperature that is regulated by CC sensitivity, which is recovered by $\gamma_{c,T}$ in our theory. The uniform MSE increase was argued by Byrne and O'Gorman (2013) as an alternative starting point, though they were focused on land–sea contrasts in warming, rather than the equator-to-pole contrast. Merlis

and Henry (2018) found that it does not satisfy energy balance with constant diffusivity, and we now show that it can be a EBM solution with a diffusivity increasing with T_0 at the rate of $\gamma_{c,h}$.

For the diffusivity that depends on temperature and MSE contrasts $\mathcal{D} = \mathcal{D}(T_2, h_2) \propto T_2^n h_2^m$ and $n \geq 0$, $m \geq 0$, the temperature gradient is always found to reduce and the MSE gradient is always found to enhance when T_0 is increased. We acknowledge that there remains an incomplete understanding of the diffusivity change with global warming, and more generally, a diffusivity theory that is well justified for moist atmospheres. However, to the extent that the general form of diffusivity considered here can capture the essence of the previously proposed theories (Held and Larichev 1996; Barry et al. 2002; Frierson et al. 2007; Chang and Held 2022; Lu et al. 2022), it is perhaps fair to expect that a changing diffusivity only modulates the amplitude but does not eliminate the polar amplification in warm climates. Relatedly, the equator-to-pole MSE contrast is always amplified, since the effect of temperature dependence of saturation specific humidity wins over the effect of temperature gradient change. Therefore, the two limiting cases of uniform temperature or MSE increase discussed in $\mathcal{D}(T_0)$ theory indeed turn out to be relevant benchmarks in thinking about the role of diffusivity changes on the pattern of warming.

Due to the opposite change of temperature and MSE gradients, the diffusivity sensitivity [internally determined by $\mathcal{D}(T_2, h_2)$] is consistently found to be bounded by $\gamma_{c,T} < \gamma < \gamma_{c,h}$. The compensating effect of the two gradients that limits the diffusivity change was speculated by Chang and Held (2022) as an explanation for why a climate-invariant diffusivity has empirically been successful in some previous EBM studies when emulating comprehensive GCM simulations. The analytic theory here provides an explicit quantitative means of evaluating this speculation. Likewise, the theory also offers a quantitative expression for a similar argument of Lu et al. (2022). Assuming a temperature gradient dependence, they argued that the diffusivity has to decrease but can only decrease moderately with warming, which they confirmed in both EBM and GCM numerical results. In our analytic theory, this is equivalent to setting $m = 0$, which gives $\gamma_{c,T} < \gamma < 0$. Therefore, the fact that the diffusivity change is limited due to dynamical constraints likely explains why the constant-diffusivity EBM in Merlis and Henry (2018) can already provide a decent estimate for polar amplification.

Finally, we emphasize that the diffusivity forms $\mathcal{D}(T_0)$ and $\mathcal{D}(T_2, h_2)$ studied here are motivated by and in hopes of making connection to previous studies. However, they are also arguably the only two relevant forms that offer feasible analytic solutions with our current EBM formulations. To ensure we obtain a diffusivity closure suitable for analytic EBM theories, we inevitably have to ignore other factors that are potentially important in determining the diffusivity

response to warming, especially the role of vertical thermal structure (O'Gorman 2011; Payne et al. 2015; Cronin and Jansen 2016; Henry and Merlis 2020; Chang and Held 2022). Additional research to arrive at formulations for the diffusivity of moist atmospheric macroturbulence in terms of the surface variables that govern EBMs or formulations for EBMs that incorporate vertical information would help further extend the thoery presented here. Also, our analytic and numerical EBM solutions assume spatially uniform feedbacks and spatially uniform diffusivity. Relaxing these assumptions individually will help bridge the remaining gap between EBM theory for temperature change in GCM simulations.

Data availability statement. The code to reproduce the numerical EBM calculations and figures is availabe at `https://github.com/cyinchang/EBM-diffusivity`.

APPENDIX

We here express the sensitivities of T_2, h_2, and $\mathcal{D}$ as functions of μ [Eq. (23)] and χ [Eq. (24)] for different diffusivity formulations. For $\mathcal{D} = \bar{\mathcal{D}}$, Eqs. (7) and (10) can be rewritten as:

$$\frac{\partial \ln T_2}{\partial T_0} = \frac{-\chi}{1+\mu}, \tag{A1}$$

and

$$\frac{\partial \ln h_2}{\partial T_0} = \frac{\chi \mu}{1+\mu}. \tag{A2}$$

For $\mathcal{D} = \mathcal{D}(T_0)$ [Eq. (2)], Eqs. (12) and (17) can be rewritten as:

$$\frac{\partial \ln T_2}{\partial T_0} = \frac{-(\chi+\gamma)}{1+\mu}, \tag{A3}$$

and

$$\frac{\partial \ln h_2}{\partial T_0} = \frac{(\chi \mu - \gamma)}{1+\mu}. \tag{A4}$$

For $\mathcal{D} = \mathcal{D}(T_2, h_2)$ [Eq. (3)], Eqs. (20), (21) and (22) can be rewritten as:

$$\frac{\partial \ln T_2}{\partial T_0} = \frac{-\chi(m+1)}{m+n+1+\mu}, \tag{A5}$$

$$\frac{\partial \ln h_2}{\partial T_0} = \frac{\chi(\mu+n)}{m+n+1+\mu}, \tag{A6}$$

and

$$\frac{\partial \ln \mathcal{D}}{\partial T_0} = \frac{\chi(m\mu - n)}{m+n+1+\mu}. \tag{A7}$$

References

Armour, K. C., N. Siler, A. Donohoe, and G. H. Roe, 2019: Meridional atmospheric heat transport constrained by energetics and mediated by large-scale diffusion. *J. Climate*, **32**, 3655–3680, https://doi.org/10.1175/JCLI-D-18-0563.1.

Barry, L., G. C. Craig, and J. Thuburn, 2002: Poleward heat transport by the atmospheric heat engine. *Nature*, **415**, 774–777.

Beer, E., and I. Eisenman, 2022: Revisiting the role of the water vapor and lapse rate feedbacks in the Arctic amplification of climate change. *J. Climate*, **35**, 2975–2988.

Bischoff, T., and T. Schneider, 2014: Energetic constraints on the position of the Intertropical Convergence Zone. *J. Climate*, **27**, 4937–4951.

Bonan, D. B., N. Siler, G. H. Roe, and K. C. Armour, 2023: Energetic constraints on the pattern of changes to the hydrological cycle under global warming. *Journal of Climate*, 1–48, https://doi.org/10.1175/JCLI-D-22-0337.1.

Byrne, M. P., and P. A. O'Gorman, 2013: Land-ocean warming contrast over a wide range of climates: Convective quasi-equilibrium theory and idealized simulations. *J. Climate*, **26**, 4000–4016.

Chang, C.-Y., and I. M. Held, 2022: A scaling theory for the diffusivity of poleward eddy heat transport based on Rhines scaling and the global entropy budget. *J. Atmos. Sci.*, **79**, 1743–1758.

Cronin, T. W., and M. F. Jansen, 2016: Analytic radiative-advective equilibrium as a model for high-latitude climate. *Geophys. Res. Lett.*, **43**, 449–457.

Crook, J. A., P. M. Forster, and N. Stuber, 2011: Spatial patterns of modeled climate feedback and contributions to temperature response and polar amplification. *J. Climate*, **24**, 3575–3592.

Feldl, N., and T. M. Merlis, 2021: Polar amplification in idealized climates: the role of ice, moisture, and seasons. *Geophys. Res. Lett.*, e2021GL094130.

Flannery, B. P., 1983: Energy balance models incorporating transport of thermal and latent energy. *J. Atmos. Sci.*, **41**, 414–421.

Frierson, D. M. W., I. M. Held, and P. Zurita-Gotor, 2007: A gray-radiation aquaplanet moist GCM. Part II: Energy transports in altered climates. *J. Atmos. Sci.*, **64**, 1680–1693.

Green, J. S. A., 1970: Transfer properties of the large-scale eddies and the general circulation of the atmosphere. *Quart. J. Roy. Meteor. Soc.*, **96**, 157–185.

Held, I. M., and V. D. Larichev, 1996: A scaling theory for horizontally homogeneous, baroclinically unstable flow on a beta-plane. *J. Atmos. Sci.*, **53**, 946–952.

Held, I. M., and B. J. Soden, 2006: Robust responses of the hydrological cycle to global warming. *J. Climate*, **19**, 5686–5699.

Henry, M., and T. M. Merlis, 2020: Lapse rate changes dominate residual polar warming in solar radiation management experiments. *Geophys. Res. Lett.*, **47**, e2020GL087 929.

Hill, S. A., N. J. Burls, A. Fedorov, and T. M. Merlis, 2022: Symmetric and antisymmetric components of polar-amplified warming. *J. Climate*, **35**, 3157–3172.

Hwang, Y.-T., and D. M. W. Frierson, 2010: Increasing atmospheric poleward energy transport with global warming. *Geophys. Res. Lett.*, **37**.

Lu, J., W. Zhou, H. Kong, L. R. Leung, B. Harrop, and F. Song, 2022: On the diffusivity of moist static energy and implications for the polar amplification response to climate warming. *J. Climate*, **35**, 3521–3540.

Merlis, T. M., 2014: Interacting components of the top-of-atmosphere energy balance affect changes in regional surface temperature. *Geophys. Res. Lett.*, **41**, 7291–7297.

Merlis, T. M., N. Feldl, and R. Caballero, 2022: Changes in poleward atmospheric energy transport over a wide range of climates: Energetic

and diffusive perspectives and a priori theories. *J. Climate*, **35**, 2933–2948.

Merlis, T. M., and M. Henry, 2018: Simple estimates of polar amplification in moist diffusive energy balance models. *J. Climate*, **31**, 5811–5824.

Mooring, T. A., and T. A. Shaw, 2020: Atmospheric diffusivity: A new energetic framework for understanding the midlatitude circulation response to climate change. *J. Geophys. Res.*, **125**, e2019JD031 206.

North, G. R., 1975: Theory of energy-balance climate models. *J. Atmos. Sci.*, **32**, 2033–2043.

North, G. R., R. F. Cahalan, and J. A. Coakley, 1981: Energy balance climate models. *Rev. Geophys.*, **19**, 91–121.

O'Gorman, P. A., 2011: The effective static stability experienced by eddies in a moist atmosphere. *J. Atmos. Sci.*, **68**, 75–90.

O'Gorman, P. A., and T. Schneider, 2008: Energy of midlatitude transient eddies in idealized simulations of changed climates. *J. Climate*, **21**, 5797–5806.

Payne, A. E., M. F. Jansen, and T. W. Cronin, 2015: Conceptual model analysis of the influence of temperature feedbacks on polar amplification. *Geophysical Research Letters*, **42 (21)**, 9561–9570.

Pithan, F., and T. Mauritsen, 2014: Arctic amplification dominated by temperature feedbacks in contemporary climate models. *Nat. Geosci.*, **7**, 181–184.

Roe, G. H., N. Feldl, K. C. Armour, Y.-T. Hwang, and D. M. W. Frierson, 2015: The remote impacts of climate feedbacks on regional climate predictability. *Nat. Geosci.*, **8**, 135–139.

Russotto, R. D., and M. Biasutti, 2020: Polar amplification as an inherent response of a circulating atmosphere: Results from the TRACMIP aquaplanets. *Geophys. Res. Lett.*, **47**, e2019GL086 771.

Schneider, T., 2006: The general circulation of the atmosphere. *Ann. Rev. Earth Planet. Sci.*, **34**, 655–688.

Shaw, T. A., and A. Voigt, 2016: What can moist thermodynamics tell us about circulation shifts in response to uniform warming? *Geophys. Res. Lett.*, **43**, 4566–4575.

Siler, N., G. H. Roe, and K. C. Armour, 2018: Insights into the zonal-mean response of the hydrologic cycle to global warming from a diffusive energy balance model. *J. Climate*, **31**, 7481–7493.

Stone, P. H., 1972: A Simplified Radiative-Dynamical Model for the Static Stability of Rotating Atmospheres. *J. Atmos. Sci.*, **29 (3)**, 405–418.

Winton, M., 2006: Amplified Arctic climate change: What does surface albedo feedback have to do with it? *Geophys. Res. Lett.*, **33**, L03 701.

Wu, Y., M. Ting, R. Seager, H.-P. Huang, and M. A. Cane, 2011: Changes in storm tracks and energy transports in a warmer climate simulated by the GFDL CM2.1 model. *Clim. Dyn.*, **37**, 53–72.